Available online at www.sciencedirect.com

ScienceDirect

Procedia CIRP 117 (2023) 7–12

www.elsevier.com/locate/procedia

19th CIRP Conference on Modeling of Machining Operations

Model-based tool design for the manufacturing of hypocycloidal internal profiles by polygon turning

Tassilo Arndt*[a], Volker Sellmeier[b], Volker Schulze[a]

[a]*wbk Institute of Production Science, Karlsruhe Institute of Technology (KIT), Kaiserstr. 12, 76131 Karlsruhe, Germany*
[b]*Index-Werke GmbH & Co. KG Hahn & Tessky, Plochinger Str. 92, 73730 Esslingen, Germany*

*Corresponding author. Tel.: +49-721-608-42455 ; fax: +49-721-608-45004. *E-mail address:* tassilo.arndt@kit.edu

Abstract

Polygon turning is a machining process for manufacturing internal and external hypocycloidal profiles, which are becoming increasingly important for shaft-hub-connections. The highly productive process can be integrated on lathe machines. Existing analytical models are not sufficient to address the main challenge when designing tools for manufacturing internal profiles. In this work a dexel-based numerical approach is presented to calculate the limits of tool design. The findings are made usable for tool design with an analogy model and are finally validated experimentally using an alternative drive system for bone screws as an example.

Keywords: geometric modeling; kinematic simulation; hypocycloidal profiles

1. Introduction

Due to their compact design with low notch stresses and high transmission capacity, as well as their self-centering effect, polygonal shaft-hub couplings are superior compared to conventional form-fitting shaft-hub connections [1]. Since the standardized polygon types P3G and P4C are complicated and costly to be manufactured with milling and grinding [2], polygon connections are still a specialized solution for small quantities. In addition to drive technology, non-round contours are also increasingly interesting for other areas of application, such as implants with bionic contours or as drive system for bone screws in medical technology.

Nomenclature

n	Number of tappets
d_a	Diameter of circumscribed circle
d_i	Diameter of inscribed circle
e	Profile eccentricity or center distance
r	Base radius or cutting circle radius
k	Shape factor
i	Transmission ratio
ω_0	Rotational speed of the tool
ω_2	Rotational speed of the workpiece
α_m	Constr. clearance angle on sec. cutting edge
t	Trust region
a, b	Half axes of the ellipse
δ	Rotation angle of the ellipse
m	Distance to the tool center
κ	Normalized shape factor
f_n, λ	Ellipsis analogy model parameter

A promising process for the production of polygonal profiles is the so-called two-spindle-non-round-lathe process [3] also known as polygon turning. It allows to manufacture inner and outer hypotrochoidal profiles (H-profiles [4]) economically and in a wide range of variants [5].

2212-8271
10.1016/j.procir.2023.03.003

In addition, machining with geometrically defined cutting edge offers advantages compared to grinding with regard to environmental aspects [6]. Due to the complex kinematics, the cutting conditions vary depending on the polygon to be manufactured [7]. Thus care must be taken when designing the tools. The established analogy model, however, does not sufficiently address the challenges of tool design for the production of internal profiles.

Therefore, in this work an approach for the numerical calculation of the geometrical limits of the tool contour is presented and made usable for tool design in CAD with an analogy model. Furthermore, the approach is experimentally validated using the example of a screw drive for bone screws.

1.1. Hypocycloidal Profiles

Hypocycloids are special cycloids, which are formed by slip-free unrolling one circle inside another [8]. They are completely defined by three quantities: Their number of tappets n, the diameter of the circumscribed circle d_a and the diameter of the inscribed circle d_i, see figure 1a). The base radius r (equation 1) and the profile eccentricity e (equation 2) can be derived from these quantities. They enter the parametric equation of the hypocycloidal profile (equation 3). For a normalized description of the shape, Maximov [7] introduces the shape factor k (equation 4), which must not exceed a n-dependent value k_{lim} (equation 5), as otherwise profile overlap will occur, see figure 1b). When k equals k_0 (equation 6), the curvature of the center of the side is zero and the profile is neither concave nor convex.

$$r = \frac{d_a + d_i}{4} \quad (1) \qquad e = \frac{d_a - d_i}{4} \quad (2)$$

$$\begin{aligned} x &= r\cos\varphi + e\cos\left[(n-1)\varphi\right] \\ y &= r\sin\varphi - e\sin\left[(n-1)\varphi\right] \end{aligned} \quad \text{with} \quad 0 < \varphi \leq 2\pi \quad (3)$$

$$k = \frac{e}{d_a} \quad (4) \qquad k_{lim} = \frac{1}{2n} \quad (5)$$

$$k_0 = \frac{1}{2\left[1 + (n-1)^2\right]} \quad (6)$$

1.2. Polygon Turning Process

Hypocycloidal profiles can be manufactured with a turning process by adding rotations around parallel axes [10]. The method is also known as two-spindle-non-round-lathe process [3]. The tool rotates in the same direction as the workpiece keeping a fixed transmission ratio i which can directly be calculated from n (equation 7). Comparable to a conventional turning tool, the tool consists of a main and a secondary cutting edge with a transition radius, see figure 2. A center distance is set between the workpiece and tool axes, which corresponds to e [7], see figure 3a). The cutting circle radius corresponds to the base radius r.

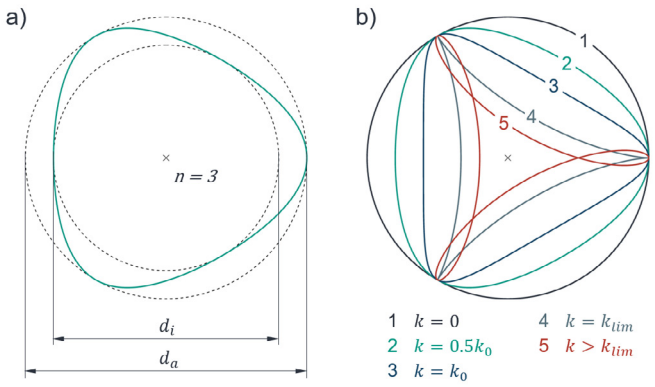

Fig. 1. (a) Hypocycloidal profiles are characterized by three quantities; (b) k allows the normalized description of the profile shape.

$$i = \frac{\omega_0}{\omega_2} = \frac{n}{n-1} \quad (7)$$

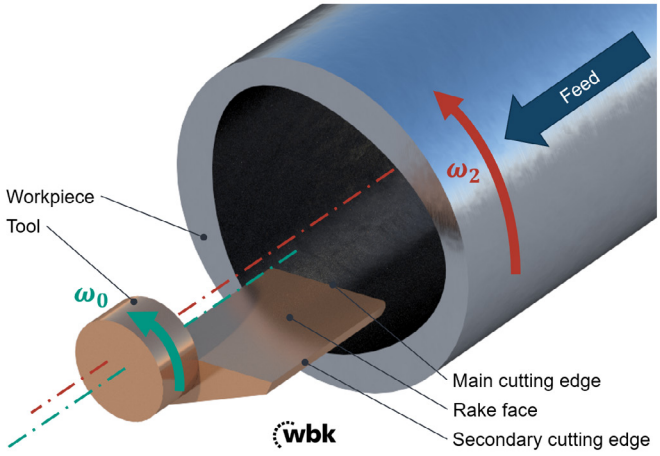

Fig. 2. Polygon turning process with simplified tool.

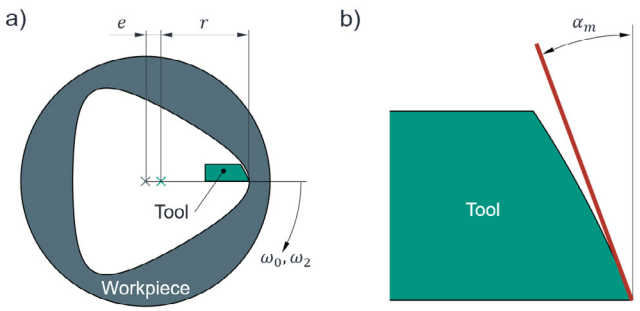

Fig. 3. (a) Process kinematics of polygon turning; (b) Mismatch between analytically calculated constructive clearance angle on secondary cutting edge and numerically calculated maximum tool shape.

Maximov [7, 9] analyses the effective rake and clearance angles on idealized main and secondary cutting edges based on mathematical considerations. Accordingly, the process is characterized by locally and temporally varying effective process parameters due to its kinematics. Especially at the secondary cutting edge, a constructive clearance angle α_m is necessary to avoid collision on the clearance surface. The angle α_m can be calculated from k and n (equation 8) using a numerically approximated angle φ^* (equation 9).

While this clearance angle enables safe tool design when manufacturing outer polygons, it is not suitable for avoiding collision at the secondary clearance surface of the tool in case of inner polygons, see figure 3b). Although α_m gives the clearance angle at the cutting tip, it significantly overestimates the actual maximal possible contour of the tool. Accordingly, clearance surface collision would occur in the process when designing only with α_m.

$$\alpha_m = \frac{\pi}{2} - \frac{\varphi^*}{n-1} - \arctan \frac{-k\cos\varphi^* + \frac{1-2k}{2(n-1)}\cos\frac{\varphi^*}{n-1}}{k\sin\varphi^* + \frac{1-2k}{2(n-1)}\sin\frac{\varphi^*}{n-1}} \tag{8}$$

$$\varphi^* = -0.007n^2 + 0.157n + 0.492 \tag{9}$$

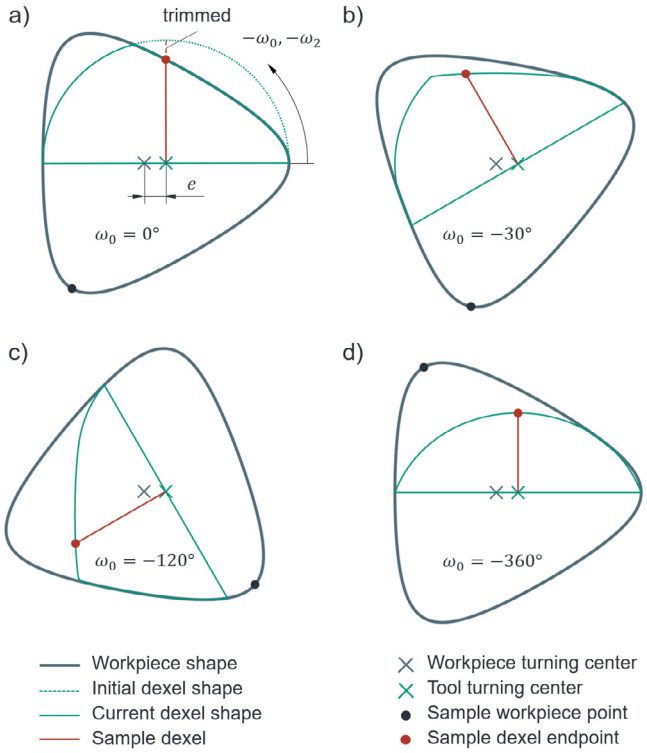

Fig. 4. Dexel-based model to calculate the maximum tool shape. (a) Initial dexel shape at $\omega_0 = 0°$; (b) $\omega_0 = -30°$; (c) $\omega_0 = -120°$; (d) Final maximum tool shape at $\omega_0 = -360°$.

2. Modeling

2.1. Dexel-Based Model

The maximum tool shape can be calculated numerically using a dexel-based model, as it is normally used for modeling subtractive manufacturing [11]. In this case, a two dimensional approach is implemented in MATLAB©. Therefore the polygon profile is modeled in the transverse section according to its parameter equation (equation 3). The initial tool shape is represented by a half circle of dexel-endpoints with its center placed e from the center of the hypocycloidal profile, see figure 4a).

Workpiece and current dexel shape representing the tool are turned using inverse kinematics and at each discrete angular step the current tool is trimmed at penetration. After one complete tool revolution, the maximum permissible tool contour is obtained, see figure 4b-d). For high geometric accuracy, a discrete resolution of 3,600 points per revolution is used.

2.2. Ellipse Analogy Model

To make the maximum tool shape usable for tool design in CAD-systems, the results of the numerical dexel-based model are generalized in an analogy model. Therefore, the calculated contour is approximated by an ellipse whose half-axes a and b as well as its rotation angle δ are to be expressed as functions of the geometric quantities of the hypocycloidal profile, see figure 5. As validity limits of the ellipse model $t = 0.25r$ and $0 < k \leq k_0$ are specified.

The center of the applied ellipse M lies on the Y-axis, whose distance to the tool center m is determined by δ (equation 10). Thus, half-axis a is a function of r and δ (equation 11). The rotation angle δ is defined as an n-dependent multiple of Maximov's constructive clearance angle α_m (equation 12). The factor f_n is determined in such a way that only positive deviations between numerical and analogy shape result in the later model to ensure that the tool design is always conservative. Therefore f_n is increased in small steps of 0.0001 starting from 1 and the deviations between the dexel and the ellipse model are calculated. As soon as the deviations are no longer negative, the factor f_n is found.

As a regression approach for the half-axis b, a third-order polynomial of the form (equation 13) is chosen with the parameters λ, which are to be selected depending on n. The form factor k is therefore normalized to the value k_0. To parameterize the approach for b, a variant calculation is carried out with the numerical dexel-based model from section 2.1. For this purpose, the number of tappets n is varied in a technically relevant range from $n = 3$ to $n = 12$ [5]. In addition, the normalized shape factor κ is varied between $\kappa = 0$ and $\kappa = 1$ in 20 steps. In all cases, the half-axis b is determined numerically so that the ellipse contains the contact point KP determined by the area of validity t, see figure 5. Subsequently, the approach for b (equation 13) is parameterized using the least square method [12]. The parameters are rounded to 4 digits after the decimal point and the ellipse analogy model is compared with the numerical dexel-based model.

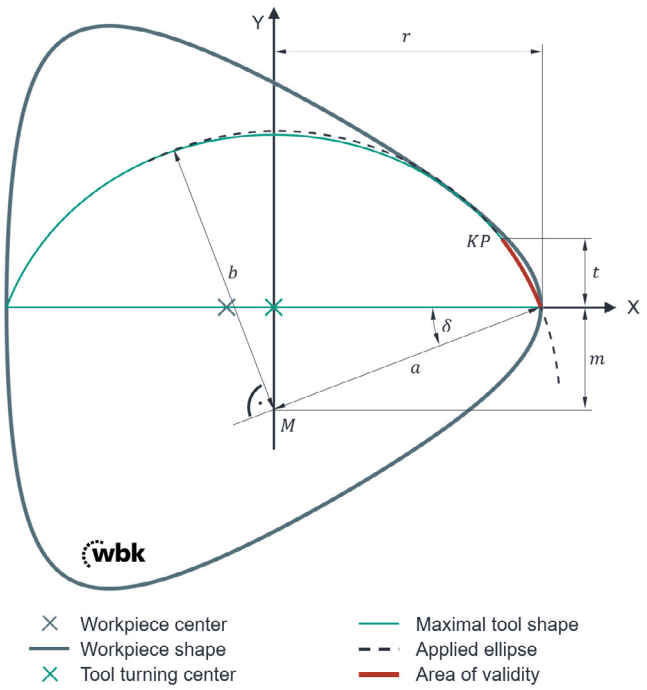

Fig. 5. Ellipse analogy model

For use in tool design, the ellipsis can be easily drawn in the CAD system. An implementation of the model for automated calculation of the model parameters is also a possibility.

$$m = -r \tan \delta \qquad (10) \qquad a = r \sqrt{\tan^2 \delta + 1} \qquad (11)$$

$$\delta = f_n \cdot \alpha_m \qquad (12)$$

$$b = d_a \left(\lambda_1 \kappa^3 + \lambda_2 \kappa^2 + \lambda_3 \kappa + 0.5 \right) \quad \text{with} \quad \kappa = \frac{k}{k_0} \qquad (13)$$

3. Experimental Setup

For the experimental validation of the ellipse analogy model, a tool is designed to perform an example process and analyze the manufactured workpiece surface as well as the clearance surface of the secondary cutting edge. As an inner contour, a superimposed triple hypocycloidal profile with enlarged inner bore is to be manufactured, as it could be used as an alternative to the conventional hexagonal profile as a drive system for bone screws, see figure 6a). The workpiece and process parameters are given in table 1. The machining tests are carried out on a Traub TNL32-7B lathe under flood cooling. At the beginning, the core drilling is made and then the two polygons are manufactured. To move out, the machine and tool are first stopped in a synchronized manner and the tool is then lifted off the surface.

In accordance with Maximov's process angle model [9], the minimum clearance angle is reached shortly after the tool enters the material, see figure 6a). To analyze the manufactured surface, the part is milled in such a way that the manufactured surfaces can be recorded with an optical surface measuring device of type Nanofocus µSurf, see figure 6b). The clearance surface of the secondary cutting edge is analyzed using a microscope of type Keyence VHX-970f.

Table 1. Workpiece and process parameters.

Parameter	Value
n	3
d_a	6 mm
d_i	3.75 mm
v_c	30 m/min
f	0.15 mm
Material	ASTM F136 (Ti6Al4V ELI)

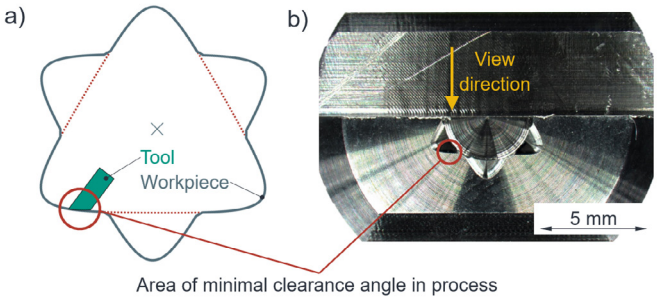

Fig. 6. Alternative bone screw drive system based on two hypocycloidal profiles: (a) Inner contour; (b) Milled part to be measured.

4. Results and Discussion

4.1. Ellipsis Analogy Model

Using the procedure from section 2.2, the resulting model parameters are given in table 2. Despite rounded parameters, the coefficients of determination of the polynomial fits are $R^2 \leq 99\%$ or better. Thus, the parameterized approximation function (equation 13) is very well able to reproduce the numerical results.

Table 2. Ellipsis analogy model parameter.

n	f_n	λ_1	λ_2	λ_3
3	1.0478	-0.1293	0.1217	-0.0899
4	1.0280	-0.0367	0.0559	-0.0439
5	1.0409	-0.0137	0.0304	-0.0054
6	1.0616	-0.0054	0.0208	0.0204
7	1.0856	-0.0010	0.0174	0.0388
8	1.1115	0.0022	0.0170	0.0526
9	1.1399	0.0056	0.0176	0.0641
10	1.1678	0.0092	0.0185	0.0735
11	1.1955	0.0131	0.0196	0.0814
12	1.2921	0.0298	0.0213	0.1027

The determined relationship between the normalized half-axis b/d_a and the normalized form factor κ, as well as the depen-

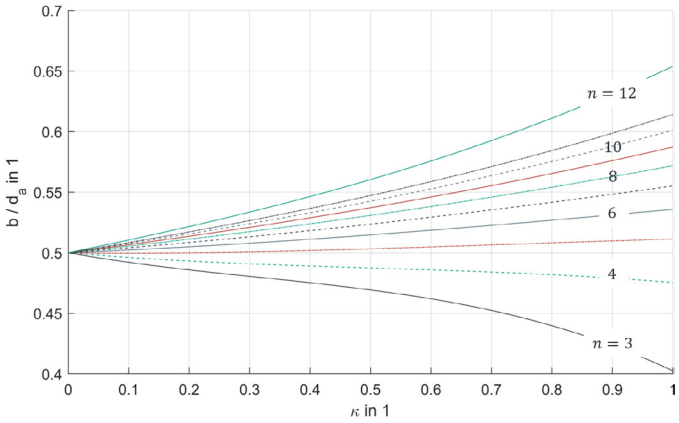

Fig. 7. Relationship for the normalized half-axis b/d_a as a function of n and κ.

dence on the number of tappets n is shown graphically in figure 7. While for hypocyclodial profiles with five tappets ($n = 5$) b corresponds approximately to $d_a/2$, b exceeds $d_a/2$ for larger n and $d_a/2$ exceeds b for smaller n.

To estimate the model error, the ellipse sections are determined with the parameterized ellipsis analogy model and then the deviations are calculated with the numerically determined contours along the contour normals. A typical deviation diagram is shown in figure 8a). Within the defined area of validity of $t/r = 0.25$, there are predominantly positive deviations, which means an underestimation of the maximum tool contour and thus a design on the safe side. Minor negative deviations occur in the range of $\kappa = 1$ and are very small compared to the exemplary assumed d_a. For the parameterized ellipsis analogy model they do not exceed 0.14 µm independent of n, see figure 8b).

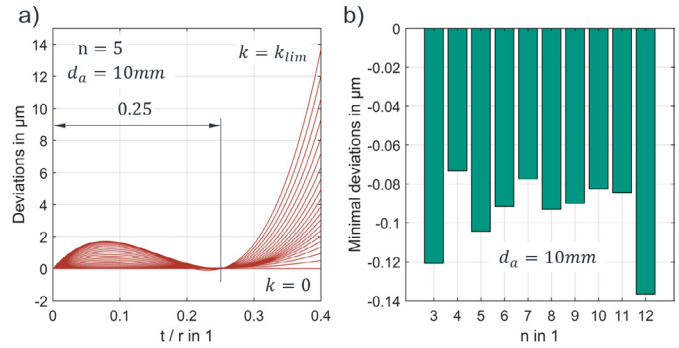

Fig. 8. Deviations of the ellipse model compared to the numerical model. Positive deviations mean an underestimation of the maximum contour. (a) Crowd of deviations for different shape factors; (b) Minimum deviations depending on n.

Outside the area of validity the deviations increase rapidly, see figure 8a). In the case of $n \leq 4$, the deviations can also turn out to be negative here. Accordingly, it is important to note the validity limits of the ellipsis analogy model.

Overall, the maximum tool contour can be approximated by the ellipse analogy model in the area of validity well. However, further boundary conditions such as distances for material springback during the process, proper chip removal and operating displacements are not considered in the model and must therefore be taken into account in tool design.

4.2. Experimental Validation

The samples for the analysis of the manufactured surfaces are taken from a series of tests in which a total of 401 components were manufactured, corresponding to 802 hypocycloidal profiles. The constructive clearance angle of the tool is derived geometrically from the ellipse model. It is chosen to be $\alpha_{\text{const.}} = 33°$, which is approx. 5° higher than calculated with α_m (equation 8).

The surfaces show no anomalies both at the beginning and at the end of the test series, see figure 9. The feed marks of the tool are clearly visible. Irrespective of the tool life, the characteristic surface parameter are $Ra = 0.478 \pm 0.069$ µm and $Rz = 3.11 \pm 0.403$ µm parallel to the feed direction. There are no indications of clearance surface interaction on the manufactured surfaces.

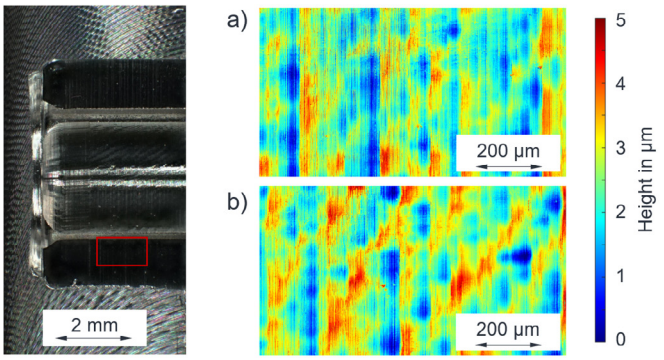

Fig. 9. False-color plots of the machined surfaces in the area of the smallest clearance angles on the secondary cutting edge. (a) Machined part 2; (b) Machined part 401.

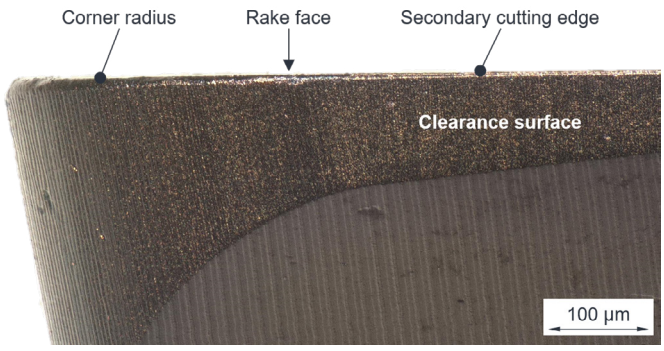

Fig. 10. View of the clearance surface of the tool on the secondary cutting edge after 401 manufactured parts.

Considering the clearance surface of the tool at the secondary cutting edge after 401 manufactured parts, no traces of clearance surface interaction can be found, see figure 10. Therefore, it is assumed that the clearance angle selected based on the

model results is sufficiently large to effectively prevent collision. The procedure for determining the maximum tool contour is therefore validated.

5. Conclusion

In this work a numerical approach for calculating the geometrical limits in tool design for polygon turning of internal contours was presented. To make the results usable for tool design in CAD-systems, an ellipse analogy model was developed and parameterized. The deviations between the determined contours were calculated and analyzed. The method was validated experimentally using a sample process and analyzing the manufactured surfaces as well as the regarding clearance surface of the tool. The following conclusions can be drawn in summary:

- For safe collision-free tool design in internal polygon turning, the maximum tool contour must be complied with.
- The numerically calculated maximum tool contour can be approximated with good accuracy using the ellipse analogy model in the specified area of validity. The maximum contour is slightly underestimated, which results in a safe tool design.
- Influencing factors such as operating displacement as well as distances for proper chip removal, springback of the material and safety are not considered in any of the models. These boundary conditions must therefore be taken into account separately.
- Due to its kinematics, the process is characterized by local and temporal changes in cutting conditions. Further work should deal with how these variations are influenced by real tool geometries, e.g. a corner radius at the transition between main and secondary cutting edges.

Acknowledgment

The research presented is funded by the German Federal Ministry of Education and Research (BMBF) within the Framework Concept “Production for medical technology - economical and of the highest quality (ProMed)” and managed by the Project Management Agency Karlsruhe (PTKA). The authors are responsible for the contents of this publication.

References

[1] Orlov, P. (1980), Fundamentals of machine design, MIR Publishers, vol. 4, pp. 69–73.
[2] Citarella, R., Gerbino, S. (2001), BE analysis of shaft-hub couplings with polygonal profiles, Journal of Materials Processing Technology,, vol. 109, pp. 30-37.
[3] Leidich, E., Reiß, F. and Schreiter, R. (2017), Investigations of hypocycloidal shaft and hub connections, Materialwissenschaft und Werkstofftechnik, vol. 48, pp. 760–766.
[4] German Institute for Standardization (2021), DIN 3689-1:2021-11, Shaft to collar connection - Hypotrochoidal H-profiles - Part 1: Geometry and dimensions, DIN e.V.
[5] Maximov, J. (2005), A new method of manufacture of hypocycloidal polygon shaft joints, Journal of Materials Processing Technology, vol. 166, pp. 144–149.
[6] Odum, K., Castillo, M., Das, J. and Linke, B. (2014), Sustainability analysis of grinding power tools, Procedia CIRP, vol. 14, pp. 570-574.
[7] Maximov, J. and Hirstov, H. (2005), Machining of hypotrochoidal surfaces by adding rotations around parallel axes, part 1: Kinematics of the method and rational field of application, Trakya University Journal of Natural Sciences, vol. 6, pp. 1–11.
[8] Schütte, F. (1902), Spezielle algebraische und transscendente ebene Kurven, Teubner, pp. 479–503.
[9] Maximov, J. and Hirstov, H. (2005), Machining of hypotrochoidal surfaces by adding rotations around parallel axes, part 1: Geometry of the body of the tool, Trakya University Journal of Natural Sciences, vol. 6, pp. 13–18.
[10] Kochsiek, A. (1997), Method and device for producing workpieces with a non-circular internal and/or external shape, patent-no WO 97/49521.
[11] Bouhadja, K. and Bey, M. (2015), Survey on simulation methods in multi-axis machining, Springer Netherlands, Berlin, p. 372.
[12] Gauss, C. (1887), Abhandlung zur Methode der kleinsten Quadrate, Verlag P. Stankiewicz, Berlin.